



## Hesperidin inhibits keratinocyte proliferation and imiquimod-induced psoriasis-like dermatitis via the IRS-1/ERK1/2 pathway



Xue Li<sup>a,b,c</sup>, Xinran Xie<sup>a,b</sup>, Lei Zhang<sup>a,b</sup>, Yujiao Meng<sup>a,b,c</sup>, Ningfei Li<sup>a,b,c</sup>, Mingxing Wang<sup>a,b</sup>, Chunyan Zhai<sup>a,b</sup>, Zhengrong Liu<sup>a,b,c</sup>, Tingting Di<sup>a,b</sup>, Lu Zhang<sup>a,b</sup>, Ping Li<sup>a,b,c,\*</sup>

<sup>a</sup> Beijing Hospital of Traditional Chinese Medicine, Capital Medical University, Beijing Institute of Traditional Chinese Medicine, Beijing 100010, China

<sup>b</sup> Beijing Key Laboratory of Clinic and Basic Research with Traditional Chinese Medicine on Psoriasis, Beijing 100010, China

<sup>c</sup> Beijing University of Chinese Medicine, Beijing 100029, China

### ARTICLE INFO

**Keywords:**  
Psoriasis  
IRS-1  
Hesperidin  
Imiquimod

### ABSTRACT

**Aims:** To evaluate the therapeutic benefits of Hesperidin (Hes) using an imiquimod (IMQ)-induced psoriasis-like mouse model and human immortalized keratinocytes (HaCaT) cells stimulated with lipopolysaccharide (LPS). **Methods:** Mice were treated with IMQ and orally administered Hes (125–500 mg/kg/day), methotrexate (MTX) 1 mg/kg/day or distilled water. HaCaT cells were stimulated with LPS (1 µg/mL) and relevant indices were measured after administration with different concentrations of Hes (5–20 µg/mL) for 24 h. Inflammatory skin lesions in IMQ mice were evaluated using the psoriasis area severity index (PASI) and pathological staining. Proteins in the IRS-1/ERK1/2 pathway and inflammatory factors were assessed using western blotting or quantitative real-time PCR. In addition, factors related to IRS-1 secretion levels were assessed by enzyme-linked immunosorbent assays. Extracellular flux (XF) analysis was used to assess cellular metabolic levels. **Key findings:** Hes significantly improved psoriasis-like skin lesions of IMQ-treated mice and inhibited LPS-induced HaCaT cell proliferation. In addition, Hes remarkably decreased PASI scores, reduced epidermal thickness, decreased proliferation and differentiation of epidermal cells, inhibited mRNA expression of inflammatory factors, reduced local skin lesions and serum insulin and glucose levels. Furthermore, Hes modulated the secretion levels of serum Leptin, Adiponectin and Resistin, and inhibited the activation of the IRS-1/ERK1/2 signaling pathway and regulated HaCaT cells metabolism. **Significance:** This study demonstrated that Hes administration could have significant therapeutic value for the prevention and clinical treatment of psoriasis.

### 1. Introduction

Psoriasis is an immune-mediated and chronic inflammatory systemic disease that results in dysfunctional epidermal homeostasis. The precise molecular pathomechanism is yet to be deciphered [1]. Previous studies have indicated that the pathogenesis of psoriasis involves the interplay of epidermal keratinocytes, T lymphocytes, leukocytes and the vascular endothelium [2]. However, there is increasing evidence that psoriasis is more than skin deep and may involve systemic dysfunctions [3]. In addition, studies have suggested that psoriasis patients are at a higher risk of developing cardiovascular and metabolic diseases including diabetes and metabolic syndrome [4]. Conversely, being overweight and obese are risk factors that exacerbate psoriasis [5,6]. Additionally, insulin has been shown to play a role in skin homeostasis. There is a strong clinical connection between psoriasis and

metabolic diseases (obesity, metabolic syndrome, etc.) that underline their pathogenesis (chronic inflammation). Insulin resistance (IR) may be one of the key driving elements [7]. Buerger et al. demonstrated that IR directly contributed to the epidermal phenotype (hyperproliferation and altered differentiation of keratinocytes) seen in psoriasis, suggesting that key cytokines inducing IR in keratinocytes and kinases mediating their effects may be attractive targets for novel anti-psoriatic therapies [8].

Hesperidin (Hes) found in tangerine peels is an ingredient of Chinese herbal medicines. It is a flavanone glycoside consisting of flavone hesperitin bound to disaccharide rutinose (Fig. 1). The various physiological properties Hes have been attributed to include: anti-inflammatory, anticancer, reducing obesity, hyperglycemia and hyperlipidemia [9–13]. Various peroxisome proliferator-activated receptor-gamma (PPAR-γ) agonists such as thiazolidinediones, a novel class of

\* Corresponding author at: NO.23, Museum Backstreet, Dongcheng District, Beijing, 100010, China.

E-mail address: [liping411@126.com](mailto:liping411@126.com) (P. Li).

<https://doi.org/10.1016/j.lfs.2019.01.019>

Received 20 October 2018; Received in revised form 6 January 2019; Accepted 14 January 2019

Available online 15 January 2019

0024-3205/ © 2019 Elsevier Inc. All rights reserved.

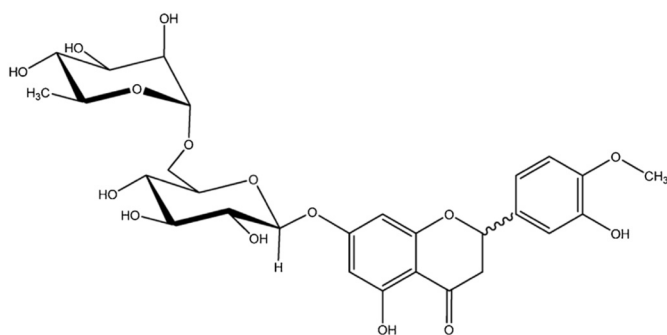


Fig. 1. Chemical structure of Hesperidin (cited from ncbi).

insulin-sensitizing drugs, have been investigated in clinical trials for psoriasis therapy [14]. Additionally, several studies have demonstrated that Hes targets PPAR- $\gamma$  [15]. Likewise, Nagashio et al. demonstrated that oral administration of Hes inhibited the production of inflammatory cytokine IL-17 and development of skin lesions. This suggested that Hes could suppress Th17 activity and enhance Treg activity [16]. A recent study demonstrated that natural compound product made from the peels of six citrus fruits may resolve psoriasis [17]. However, detailed studies investigating the role of Hes in psoriasis are lacking.

In this study, we investigate whether oral administration of Hes could alleviate psoriasis-like skin lesions in mouse model and affect epidermal keratinocyte proliferation.

## 2. Materials and methods

### 2.1. Mouse model for imiquimod (IMQ)-induced psoriasis-like skin inflammation

Male mice BALB/c (18–20 g, 8 weeks) were purchased from Beijing Huafukang Biotechnology Co., Ltd. Experimental procedures strictly followed all local ethics procedures for animal studies. Mice were randomly divided into six groups of eight mice each. The groups included the control, model, methotrexate (MTX) (1 mg/kg/day), Hes (Beijing Solarbio Science & Technology Co., Ltd., China) 500 mg/kg/day, Hes 250 mg/kg/day, and Hes 125 mg/kg/day. Hes and MTX was dissolved in pure water and administered to mice in the Hes or MTX group respectively, while pure water was administered to the control and model group. Vaseline was applied to mice in the control group while mice in the other groups received a daily topical dose of commercially available IMQ cream at 62.5 mg (Sichuan Mingxin Pharmaceutical Co., Ltd., China). This topical treatment was applied for six consecutive days on the shaved dorsal areas as described previously [18].

### 2.2. Cell culture conditions

The spontaneously immortalized human keratinocyte cell line (HaCaT) (cell culture center, Institute of Basic Medical Sciences Chinese Academy of Medical Sciences) was cultured in minimum Eagle's medium with 10% fetal calf serum (Gibco Company, USA) at 37 °C in 5% CO<sub>2</sub> atmosphere. Cells were centrifuged after digestion with 0.25% trypsin, then discard the supernatant and resuspend the medium, and the cell concentration was adjusted to inoculate the plate.

### 2.3. Psoriasis area and severity index (PASI)

A scoring system based on the clinical PASI was used to rate the macroscopic appearance of skin in the mouse models. Each of the following three conditions, i.e. erythema, infiltration, and scaling, were scored separately as 0 (not present), 1 (mild), 2 (moderate), or 3

(severe). Values from the three conditions were totaled and an integrated trend line for each group was drawn.

### 2.4. Histological and immunofluorescent staining

Paraffin sections were stained with hematoxylin and eosin (HE). Electron microscopy (IMAGER Z2, Zeiss, Germany) images of histopathological changes were recorded. Epidermal thickness was measured using the ZEN image analysis system.

Paraffin sections and cell slides ( $4 \times 10^3$ ) were stained with IRS-1 (1:100 dilution, Santa, Cat. SC-8038), ERK (1:100 dilution; CST, Cat.9102S), and phospho-ERK antibodies (1:100; CST, Cat.9101S). Sections were observed by light and fluorescence microscopy (IMAGER Z2, Zeiss, Germany).

### 2.5. Assessment of cell proliferation

The effects of Hes on LPS-induced HaCaT cell proliferation were assessed by seeding cells ( $8 \times 10^4$ ) onto 96-well plates. Cells were treated with Hes (20, 10, or 5  $\mu\text{g}/\text{mL}$ ) plus LPS (1  $\mu\text{g}/\text{mL}$ , Sigma, Cat. L4391) or NT157 (3  $\mu\text{M}$ , Selleck, Cat. S8228) plus LPS for 24 h. Negative control and LPS treated cells were included in cell proliferation assessments. The next day, 10  $\mu\text{L}$  of Cell Counting Kit-8 reagent (CCK-8, Dojindo, Japan) was added. Optical density (OD) was measured using a microplate reader at 450 nm after incubation of the CCK-8 reagent for 2 h.

### 2.6. Extracellular flux (XF) analysis

HaCaT cells were seeded onto XF 24-well cell culture microplates (Seahorse Bioscience, North Billerica, MA, USA) in triplicate at  $6 \times 10^4$  cells/well resuspended in 150  $\mu\text{L}$  growth medium and then incubated at 37 °C and 5% CO<sub>2</sub>. On the following day, cells were treated as described in Section 2.5 of the Materials and methods. 24 h post-treatment, growth media was replaced with pre-warmed (37 °C) assay media (500  $\mu\text{L}$ ). The cells were incubated at 37 °C for 30 min to allow temperature and pH of the media to reach equilibrium before initiating extracellular flux measurements. Based on the manufacturer's protocol, drugs were dispensed to the dosing port of the XF24 Analyzer. Cell mitochondrial stress analysis dosing sequence and the various drug concentrations were as follows; port A: 1  $\mu\text{M}$  oligomycin, port B: 0.5  $\mu\text{M}$  FCCP, port 0.5  $\mu\text{M}$  rotenone/antimycin A. The dosing and drug concentrations were as follows; port A: 0.5  $\mu\text{M}$  rotenone/antimycin A, port B: 50 mM 2-DG. The oxygen consumption rate (OCR) and extracellular acidification rate (ECAR) reflecting the cellular metabolic activity and cell number were measured.

### 2.7. ELISA

The serum concentrations of glucose, insulin, adiponectin, leptin and resistin were measured using the Mouse Glucose Quantitative determination kits (Biokits Tech Inc., China), Mouse Insulin ELISA kits (ExCell Biotech (Taicang) Co., Ltd., China), Mouse adiponectin/Acrp30 ELISA kits (4A Biotech Co., Ltd., China), Mouse Leptin ELISA kits (ExCell Biotech (Taicang) Co., Ltd., China) and Mouse Resistin ELISA kits (ExCell Biotech (Taicang) Co., Ltd., China) respectively. ELISA was performed based on the suggested manufacturer's protocol.

### 2.8. Real-time quantitative PCR (RT-qPCR)

Total RNA was extracted from mouse skin samples using the RNeasy Mini Kit (Qiagen). RNA was then reversed transcription to cDNA using the QuantiTect Reverse Transcription Kit. RT-qPCR was performed in triplicate or quadruplicate using the QuantiTect SYBR Green RT-qPCR Kit (Qiagen, Hilden, Germany) performed on the 7500 Real Time PCR System (Applied Biosystems, Thermo Fisher, USA). The qPCR cycling

conditions were as follows: 95 °C 5 min, (95 °C 10 s, 60 °C 30 s) 45 cycles. Gene expression levels were normalized to  $\beta$ -actin by using the  $2^{-\Delta\Delta Ct}$  method. All primers used for RT-qPCR are shown in Tables 1 and 2.

### 2.9. Western blotting analysis

Total protein from skin lesions or HaCaT cells from each treatment group was extracted using RIPA buffer supplemented with PMSF. Total protein was quantified using the bicinchoninic acid (BCA) protein assay method. Equal amounts of protein from each treatment group were separated on a 12% SDS-PAGE gel and then transferred to a nitrocellulose (NC) filter membrane. Membranes were blocked with 3% bovine serum albumin and then incubated with the relevant primary antibody. After primary antibody incubation, the membranes were washed with TBS-T and then incubated with the appropriate secondary antibody. Protein bands were detected using chemiluminescence. Band intensities were quantified using Image J software. GAPDH was used as the loading control. All antibodies that were used in this study are listed in Tables 3 and 4.

### 2.10. Statistical analysis

Statistical analyses were performed using one-way analysis of variance (ANOVA) for the different groups. Differences were considered statistically significant at  $p < 0.05$ . All data were expressed as “mean  $\pm$  SD”.

## 3. Results

### 3.1. Psoriasis-like lesions improved in mice after Hes administration

Skin scaling, erythema and inflammatory infiltrates appeared after the 7th day of modeling. Mice treated with Hes had similar skin morphology as to mice in the MTX group, which had smoother skin, few scales, superficial erythema, and reduced inflammation and skin thickening (Fig. 2A). Based on the daily PASI scores, the skin lesions became more severe on each subsequent day of IMQ application in the model group. There was more immune infiltration, erythema that developed from pale pink spots to large areas of deep red plaques, and skin scaling was thick and widely distributed. However, the PASI total scores for mice in Hes (500 mg/kg and 250 mg/kg) groups were reduced and were almost similar to mice in the MTX group. And the effect of Hes (125 mg/kg) group was slightly weaker than that of other doses, but it could also significantly improve the skin lesion. The higher concentration of Hes, the effect on improving scales closer to MTX group. On the 5th day after orally administration of Hes (500 mg/kg and 250 mg/kg) group, improvement infiltration and visibly reduced scaling was observed, and the effect was even stronger than MTX group. And the effect of Hes (125 mg/kg) group also surpassed that of MTX group on the 6th day. Concurrently, the color of the erythema gradually lightened after oral administration of Hes and the effect was better than MTX group on the 2nd day (Fig. 2B).

To further evaluate the effects of Hes in IMQ-induced psoriasis-like mouse models, we conducted histopathological analysis by HE staining from dorsal skin samples in mice from each group. In the model group, the epidermal acanthocyte layer was thickened, the stratum corneum was keratinized, infiltration of inflammatory cells in the dermis was obvious, and the digitation of the epidermis was downward. The thickness of the epidermis was significantly ascended compare to the control group. The histological appearance was similar to that of psoriatic lesions. The skin layer of mice in the Hes treated group was thinner, hyperkeratosis and parakeratosis were reduced, inflammatory cells in the dermis were reduced, the dermis was thinner and the thickness of the epidermis was decreased significantly (Fig. 2C and D). These manifestations Hes significantly reduced the thickness of the

epidermis, reduced the pathological changes and attenuated IMQ-induced psoriasis.

### 3.2. Hes administration inhibited the proliferation and differentiation of keratinocytes in the psoriasis-like mouse model

PCNA is an important indicator for cell mitosis. It was measured to determine the proliferative rate of keratinocytes in mice. Using immunofluorescence staining, the number of epidermal cell layers covering almost the entire epidermis of mice in the model group was significantly increased (Fig. 3A). The number of mitotic cell nuclei (the number of positive nuclei with PCNA), the number of total nuclei (the number of nuclei with DAPI staining) and the ratio of mitotic positive cells was significantly elevated in mice from the model group compared to mice in the control group. However, the number of epidermal cells on the basal layer had the tendency to be linearly distribution with each dose Hes group reduced. The number of mitotic cells, total nuclei and the ratio of mitotic positive cells were dramatically reduced compared to mice in the model group (Fig. 3B and Fig. S1).

In addition, Involucrin was measured to evaluate keratinocyte differentiation in mice from each treatment group. The integrated optical density (IOD) values for the model group were widely distributed, highly expressed, and with a large epidermal expression area (Fig. 3C). The IOD values for each Hes dose group were localized in the strata corneum epidermidis and upper spinous layer. Hes treated mice had reduced involucrin expression levels with decreased expression areas (Fig. 3D). Hence, Hes effectively reduced IMQ-induced keratinocyte proliferation and ameliorated the abnormal differentiation of epidermal cells and IMQ-induced keratinocyte differentiation.

### 3.3. Hes decreases pro-inflammatory cytokines in the psoriasis-like mouse model

Increased expression levels of pro-inflammatory cytokines were observed in IMQ-induced lesions. Although Hes did not significantly inhibit IL-6 mRNA expression levels, IL-17, IL-23 and IL-22 mRNA levels for mice in each Hes-dosed groups were significantly decreased in a dose-dependence manner. In addition the relative IL-1 $\beta$  expression levels in mice from the Hes (500 and 250 mg/kg)-dosed groups were reduced, while the relative TNF- $\alpha$  mRNA expression levels in mice from the Hes (500 mg/kg)-dosed group was lower compared to mice in the model group (Fig. 4).

### 3.4. Hes inhibits IRS-1 expression and phosphorylation of ERK1/2 protein in IMQ-induced psoriasis-like skin lesions

To investigate the role of Hes in the IRS-1/ERK1/2 pathway, we measured the expression levels of ERK1/2 and IRS-1 in IMQ-induced psoriasis-like skin lesions by immunofluorescence, RT-qPCR and western blot. Immunofluorescence analysis showed that the IOD values for IRS-1 and p-ERK1/2 in the skin lesions of mice in the model group were significantly increased (Fig. 5A and D, Figs. S2A and S3A). Similar results using qPCR and western blotting were found for IRS-1 mRNA and protein expression (Fig. 5B and C, Fig. S3B), as well as for phosphorylated ERK1/2 (Fig. 5E). The ratio of p-ERK1/2 to total ERK1/2 protein levels were increased in mice from the model group (Fig. S3B). However, after treatment with Hes, the IOD values and relative expression levels of IRS-1 in the lesions of mice were decreased. In addition, IOD values of p-ERK1/2 in the skin lesions of mice treated with Hes was decreased to a certain extent. The levels of p-ERK1/2 were reduced in the skin lesions of mice treated with Hes at both 500 and 250 mg/kg doses. In addition, the ratio of p-ERK1/2 to total ERK1/2 protein levels was decreased.

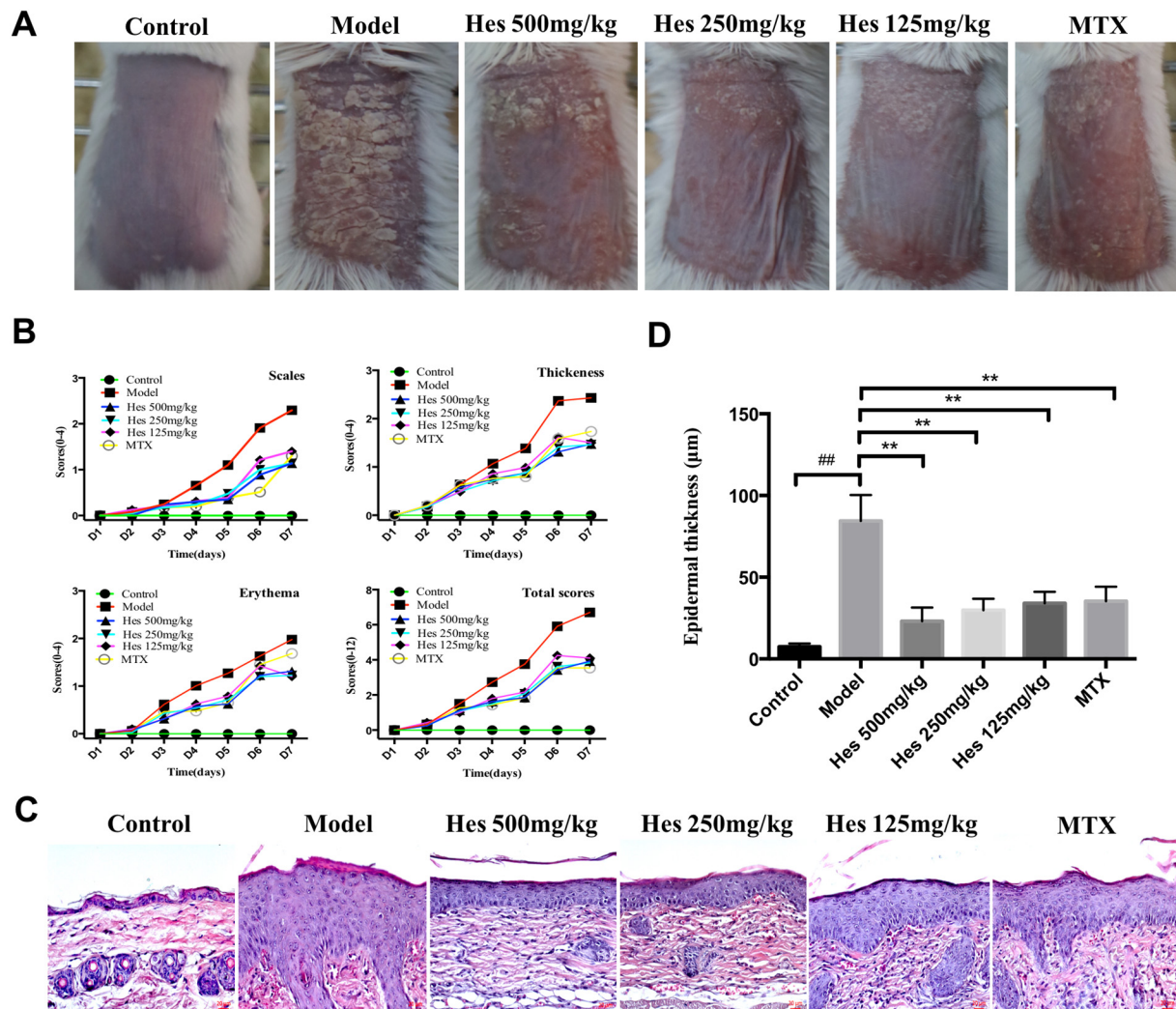


**Fig. 2.** The morphology of Imiquimod (IMQ)-induced psoriasis form dermatitis in mouse models. (A) Images from each group on the seventh day. (B) Psoriasis area and severity index (PASI) scores in the control, model, Hes (500 mg/kg/day), Hes (250 mg/kg/day), Hes (125 mg/kg/day) and MTX treated mice. (C) Skin biopsies were stained with hematoxylin and eosin (H&E,  $\times 400$ ). Scale bar = 20  $\mu\text{m}$ . (D) Epidermal thickness was measured using the image analysis system. Data are expressed as the mean  $\pm$  SD ( $n = 6$ ).  $*p < 0.05$  and  $**p < 0.01$  vs the model group;  $\#p < 0.05$  and  $\#\#p < 0.01$  vs the control group. (For interpretation of the references to color in this figure, the reader is referred to the web version of this article.)

### 3.5. Hes regulates insulin levels in skin lesions and serum; and levels of serum glucose

Insulin levels in psoriatic lesions and serum; and serum glucose in IMQ-induced psoriasis mice were examined to investigate the effect of Hes on IRS-1. While serum insulin levels in mice from the model group had a slight decline, the insulin mRNA expression levels in the skin lesions were significantly decreased (Fig. 6A). Serum insulin levels in mice treated with Hes were similar, except in mice treated with Hes (500 mg/kg) that showed a slight increase (Fig. 6B). However, administration of Hes had an obvious effect in increasing the relative expression of insulin mRNA in skin lesions. This was especially obvious in mice treated with Hes (500 mg/kg and 125 mg/kg) and showed statistical significance. Conversely, the serum glucose levels of mice in the model group declined substantially. Besides, mice administered with Hes (500 mg/kg) were able to upregulate their serum glucose levels (Fig. 6C).

### 3.6. Regulation of serum leptin, resistin and adiponectin levels by Hes

In the model group, serum leptin and adiponectin levels declined while serum resistin levels increased substantially. However, after

administration of Hes (500 or 250 mg/kg), there was significant upregulation of leptin and adiponectin levels, while resistin levels decreased. In mice treated with Hes (125 mg/mg), leptin and resistin levels were slightly increased, while adiponectin levels were still enhanced (Fig. 6D).

### 3.7. Hes regulates phosphorylation on different sites of IRS-1 and ERK1/2 to inhibit LPS-induced proliferation in HaCaT

Hes at different concentrations could inhibit LPS-induced cell proliferation to varying degrees. The inhibitory effect of Hes on LPS-induced cell proliferation reached its peak at 24 h, and was inhibited in a dose-dependent manner (Fig. 7A). Concurrently immunofluorescence staining, RT-qPCR and western blot analysis was performed at that timepoint. IRS-1 mRNA expression was increased after LPS treatment (Fig. 7B). In addition, after treatment with NT157, cell proliferation was reduced in cells treated with LPS at 24 h (Fig. 7A).

After 24 h of LPS stimulation, IRS-1 was highly expressed as detected by immunofluorescence assays. In addition, positive staining for p-ERK1/2 was observed in HaCaT on the cell membrane, cytoplasm and nucleus, while there was almost no staining in the control cells, with only positive staining on the membrane and weak staining in the

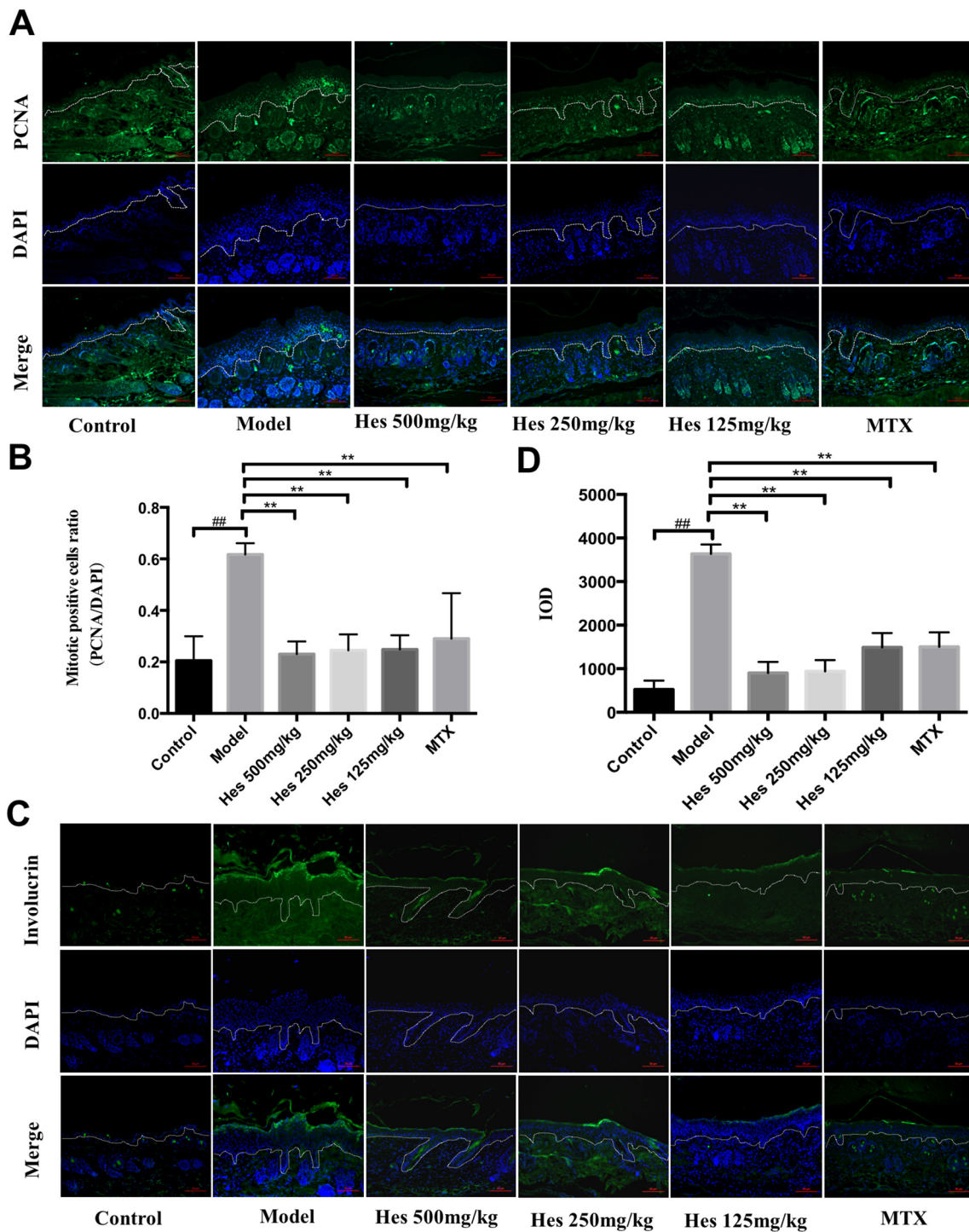


**Fig. 3.** Epidermal cell proliferation and differentiation of IMQ-induced psoriasiform dermatitis in mouse models. (A) Immunofluorescence (IF,  $\times 200$ ) images of epidermal cell proliferation in mice skin. PCNA (green), DAPI (blue) and merge. Scale bar = 50  $\mu\text{m}$ . (B) The ratio of PCNA positive cells to DAPI denoting number of cells in mitosis. Data are expressed as the mean  $\pm$  SD (n = 6). \* $p < 0.05$  and \*\* $p < 0.01$  vs the model group; # $p < 0.05$  and ## $p < 0.01$  vs the control group. (C) Immunofluorescence (IF,  $\times 200$ ) images of epidermal cell differentiation in mice skin. Involverin (green), DAPI (blue) and merge. Scale bar = 50  $\mu\text{m}$ . (D) The IOD values of Involverin were measured using the image analysis system. Data are expressed as the mean  $\pm$  SD (n = 6). \* $p < 0.05$  and \*\* $p < 0.01$  vs the model group; # $p < 0.05$  and ## $p < 0.01$  vs the control group. (For interpretation of the references to color in this figure legend, the reader is referred to the web version of this article.)

cytoplasm and nucleus (Fig. 7C and E). The protein relative expression of IRS-1, p-ERK1/2, and the ratio of p-ERK1/2 to ERK1/2 were also increased in cells treated with LPS as analyzed by western blots. IRS-1 mRNA and protein expression was down-regulated after treatment with different concentrations of Hes, particularly at a dose of 20  $\mu\text{g}/\text{mL}$ . However, NT157 treatment had not effect. After Hes treatment, the

relative protein expression of p-ERK1/2 decreased in a dose-dependent manner. The ratio of p-ERK1/2 to ERK1/2 declined, especially at Hes doses of 10 and 5  $\mu\text{g}/\text{mL}$ . NT157 only weakly reduced the relative expression of p-ERK1/2 but had no effect on the ratio of p-ERK1/2 to ERK1/2 (Fig. 7D and F).

In addition, we examined the IRS-1 phosphorylation levels at

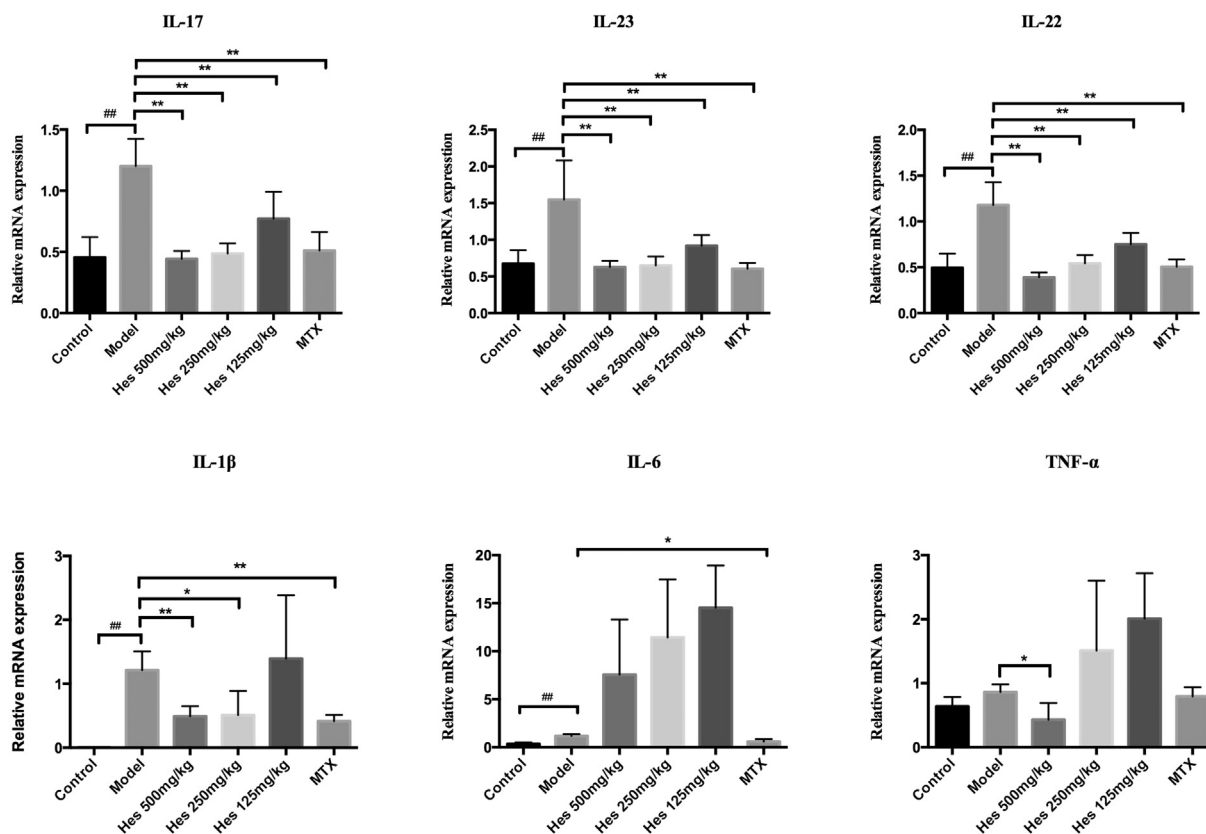


Fig. 4. The relative gene expression levels of IL-17, IL-23, IL-22, IL-1 $\beta$ , IL-6 and TNF- $\alpha$  in the skin of mice as determined by RT-qPCR. Graphs indicate the mean  $\pm$  SD for each group (n = 6). \* $p$  < 0.05 and \*\* $p$  < 0.01 vs the model group; # $p$  < 0.05 and ## $p$  < 0.01 vs the control group.

different sites in LPS-stimulated HaCaT cells. We found that the relative expression levels of p-IRS-1 (Tyr612) and p-IRS-1 (Ser312) were slightly increased after LPS stimulation. The ratio of p-IRS-1 (Ser312) to IRS-1 increased, while the ratio of p-IRS-1 (Tyr612) to total IRS-1 decreased. Hes treatment after LPS stimulation decreased relative protein expression of p-IRS-1 (Ser312), p-IRS-1 (Tyr612) and the ratio of p-IRS-1 (Ser312) to IRS-1. The ratio of p-IRS-1 (Tyr612) to IRS-1 decreased with increasing concentrations of Hes. In addition, NT157 decreased the relative expression of p-IRS-1 (Ser312), p-IRS-1 (Tyr612) and the ratio of p-IRS-1 (Ser312) to IRS-1, however the ratio of p-IRS-1 (Tyr612) to IRS-1 was unchanged (Fig. 7D).

### 3.8. Effect of Hes on aerobic respiration and cell proliferation

Seahorse was used to measure metabolism in LPS-stimulated HaCaT cells treated with various concentrations of Hes. The results showed that HaCaT cells mainly undergo aerobic respiration after LPS stimulation. The baseline mitochondrial respiration levels and ATP production was measured. Aerobic respiration was measured after adding oligomycin, Carbonyl cyanide-p-trifluoromethoxy phenylhydrazone (FCCP), or Rotenone/Antimycin A. LPS significantly increased respiration and addition of Hes decreased these values (Fig. 8). We also investigated the glycolysis pathway in HaCaT cells after LPS stimulation. The baseline extracellular acid production capacity, the maximum after adding Rotenone/Antimycin A and even addition of 2-DG (inhibits the breakdown of glucose to reduced extracellular acid production) were slightly higher after LPS stimulation. However, the overall change was minimal (Fig. S4). We observed that the baseline respiratory levels and ATP production capacity for each Hes concentration was higher, especially for Hes at 20  $\mu$ g/mL, which was the most significant. The maximum mitochondrial respiration levels in HaCaT cells treated with different concentrations of Hes were also reduced to a certain extent.

The maximum respiration levels reduced with increasing concentrations of Hes. In addition, the respiratory capacity reserve values of the cells for the different concentrations of Hes were also lower compared to LPS stimulated cells, especially at doses of 20  $\mu$ g/mL and 10  $\mu$ g/mL.

## 4. Discussion

Epidemiological and clinical studies have demonstrated that the prevalence of metabolic syndromes in patients with psoriasis is higher compared to non-psoriasis patients [19,20], and has become a potential risk factor that affects the quality of life in patients [21]. IR is frequently observed in psoriasis patients with metabolic diseases and is closely associated with metabolic and immune disorders [22,23]. Previously studies have shown that Hes alleviates IR both in vitro and in vivo [9]. MTX has therapeutic efficacy on psoriatic lesions [24]. Our present findings suggest that Hes could effectively alleviate IMQ-induced psoriasis-like symptoms such as thickening, skin scaling and erythema. And the therapeutic benefit for mice in Hes was equivalent to that of MTX. Hes could also reduce excessive proliferation and differentiation of skin lesions in a dose-dependent manner. In fact, it has been reported that Hes inhibits tumor cell proliferation in a time-dosage dependent manner [25]. Hes inhibited mitosis in epidermal cells and reduced excessive proliferation in epidermal cells in psoriasis-like lesions. In vitro, we found that LPS could induce proliferation of HaCaT cells. With prolonged stimulation, the OD values increased, especially after cells were stimulated for 24 h. Hes suppressed proliferation of HaCaT cells induced by LPS, and was dose-dependent. In addition to its inhibitory effect on epidermal cell proliferation, Hes also affected the differentiation of epidermal cells, suggesting that topical Hes application could help improve epidermal barrier function [26]. Studies on the anti-inflammatory functions of Hes have been actively investigated. In previous studies, Hes substantially reduced the levels of inflammatory

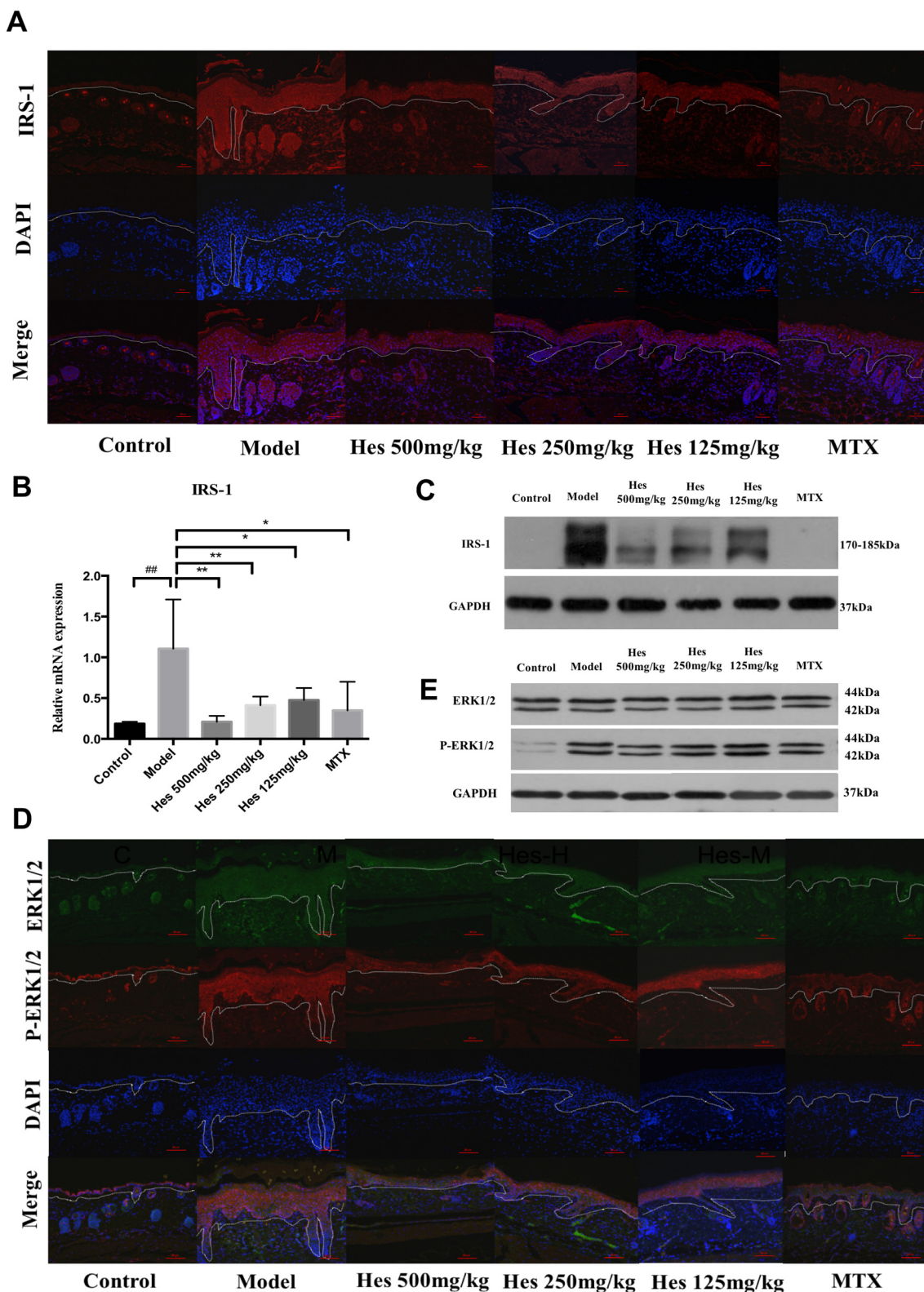


**Fig. 5.** Expression of IRS-1, ERK1/2, p-ERK in the skin of mice. (A) Immunofluorescence (IF,  $\times 200$ ) images of IRS-1 in mouse skin. IRS-1 (red), DAPI (blue) and merge. Scale bar = 50  $\mu\text{m}$ . (B) The relative levels of IRS-1 gene expression in the skin of mice as determined by RT-q PCR. Graphs indicate the mean  $\pm$  SD for each group (n = 6). \* $p < 0.05$  and \*\* $p < 0.01$  vs the model group; # $p < 0.05$  and ## $p < 0.01$  vs the control group. (C) Protein levels of IRS-1 in the skin of mice. GAPDH was used to confirm equal amount of protein (n = 3). (D) Immunofluorescence (IF,  $\times 200$ ) images of ERK1/2 and p-ERK1/2 in mouse skin. ERK1/2 (green), p-ERK1/2 (red), DAPI (blue) and merge. Scale bar = 50  $\mu\text{m}$ . (E) Protein levels of ERK1/2, p-ERK1/2 in the skin of mice. GAPDH was used to confirm equal amount of protein (n = 3). (For interpretation of the references to color in this figure legend, the reader is referred to the web version of this article.)

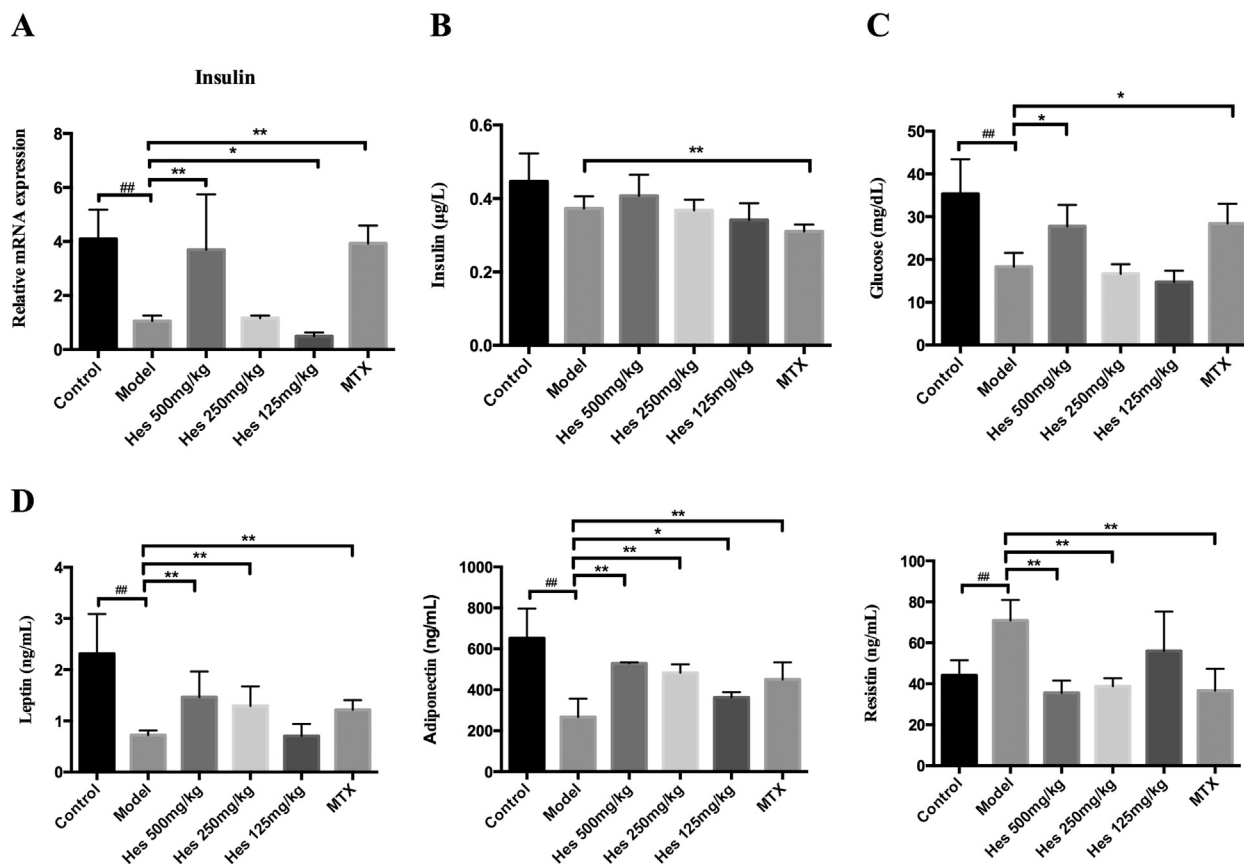


**Fig. 6.** Secretion levels of factors related to IRS-1 in skin or serum of mice. (A) The relative levels of insulin gene expression in the skin of mice were determined by RT-q PCR. Graphs indicate the mean  $\pm$  SD for each group (n = 6). \* $p$  < 0.05 and \*\* $p$  < 0.01 vs the model group; # $p$  < 0.05 and ## $p$  < 0.01 vs the control group.

(B) Insulin levels ( $\mu$ g/L) in serum using ELISA. Results are shown as mean  $\pm$  SD (n = 4). \* $p$  < 0.05, \*\* $p$  < 0.01. (C) Glucose levels (mg/dL) in serum. Results were shown as the mean  $\pm$  SD (n = 4). \* $p$  < 0.05 and \*\* $p$  < 0.01 vs the model group; # $p$  < 0.05 and ## $p$  < 0.01 vs the control group. (D) Leptin (ng/mL), Adiponectin (ng/L) and Resistin (ng/L) levels in serum. Results were shown as the mean  $\pm$  SD (n = 4). \* $p$  < 0.05 and \*\* $p$  < 0.01 vs the model group; # $p$  < 0.05 and ## $p$  < 0.01 vs the control group.

cytokines such as tumor necrosis factor alpha (TNF- $\alpha$ ), interleukin-6 (IL-6) and interleukin-1 $\beta$  (IL-1 $\beta$ ) in LPS-induced respiratory inflammatory mouse models [27], and significantly reduced IL-17 and IL-6 production by Treg cells in multiple sclerosis mouse model [28]. We also found that Hes reduced the pathological changes observed in psoriasisform dermatitis by reducing localized inflammatory cytokine expression in skin lesions.

ERK1/2 has been shown to be highly expressed in both psoriatic lesions and human keratinocytes [29,30]. IMQ and LPS could enhance the expression of ERK1/2 phosphorylation in mice skin lesions and HaCaT cells. And Hes inhibits ERK1/2 phosphorylation in vitro and in vivo. High expression of IRS-1 has also been observed in psoriatic lesions [31]. Hes reduced the increased levels of IRS-1 and ERK1/2 phosphorylation in IMQ mice skin lesions and in LPS-induced HaCaT cells in a dose-dependent manner. Previous studies have demonstrated that IRS-1 phosphorylation is critical for the activation or inhibition of its downstream signaling proteins [32]. IRS-1 Ser312 phosphorylation inactivates IRS-1, and IRS-1 Tyr612 dephosphorylation inhibits insulin intracellular signaling, which eventually leads to IRS-1 degradation and IR [33]. Interestingly, we demonstrated that Hes had different regulatory effects on the phosphorylation levels of IRS-1 at the different phosphorylation loci. Hes restored the phosphorylation of IRS-1 Tyr612, reduced the phosphorylation levels of IRS-1 Ser312, which subsequently affected intracellular signal transmission and inhibited the proliferation of LPS-induced HaCaT cells. In addition, IRS-1 a key signaling molecule in the MAPK/ERK pathway, mediates insulin

metabolism in peripheral tissues, cell proliferation and differentiation and glucose metabolism. Additionally, IRS-1 is an important signaling protein. It could effect on  $\beta$ -cell function which inhibits calcium ion ATPase in the endoplasmic reticulum and increase intracellular calcium ion concentrations to activate protein kinase C to stimulate insulin release [34]. Several studies have demonstrated that inflammatory adipokine levels (leptin, resistin, omentin, chemokine and IL-6) and IR index were increased in patients with psoriasis, and were positively correlated with the severity of psoriasis. The anti-inflammatory adipokines, adiponectin and insulin sensitivity index were lower in psoriasis compared to control and were negatively correlated with the severity of psoriasis [35,36]. Bulur et al. demonstrated that serum lipid levels were associated with the pathogenesis of psoriasis [37]. Hes significantly regulated the levels of serum insulin, leptin, adiponectin and resistin in mice. Although the effect on serum insulin levels was minimal, high doses of Hes was found to regulate serum glucose levels. We hypothesized that Hes may have treatment efficacy for psoriasis by regulating the levels of adipokines. However, from in vitro experiments, we found that Hes reduced the increased proliferation of HaCaT cells by affecting aerobic respiration. Further experimental studies are needed to determine whether the glycolysis pathway is modulated by Hes.

In our study we also used NT157, a selective IRS-1/2 inhibitor as an in vitro positive control. Cells treated with NT157 had a dose-dependent inhibition of IRS protein expression and enhanced ERK activation. Through a negative feedback regulation of IGF1R signaling, NT157 could target IRS-1/2 for serine phosphorylation and degradation to

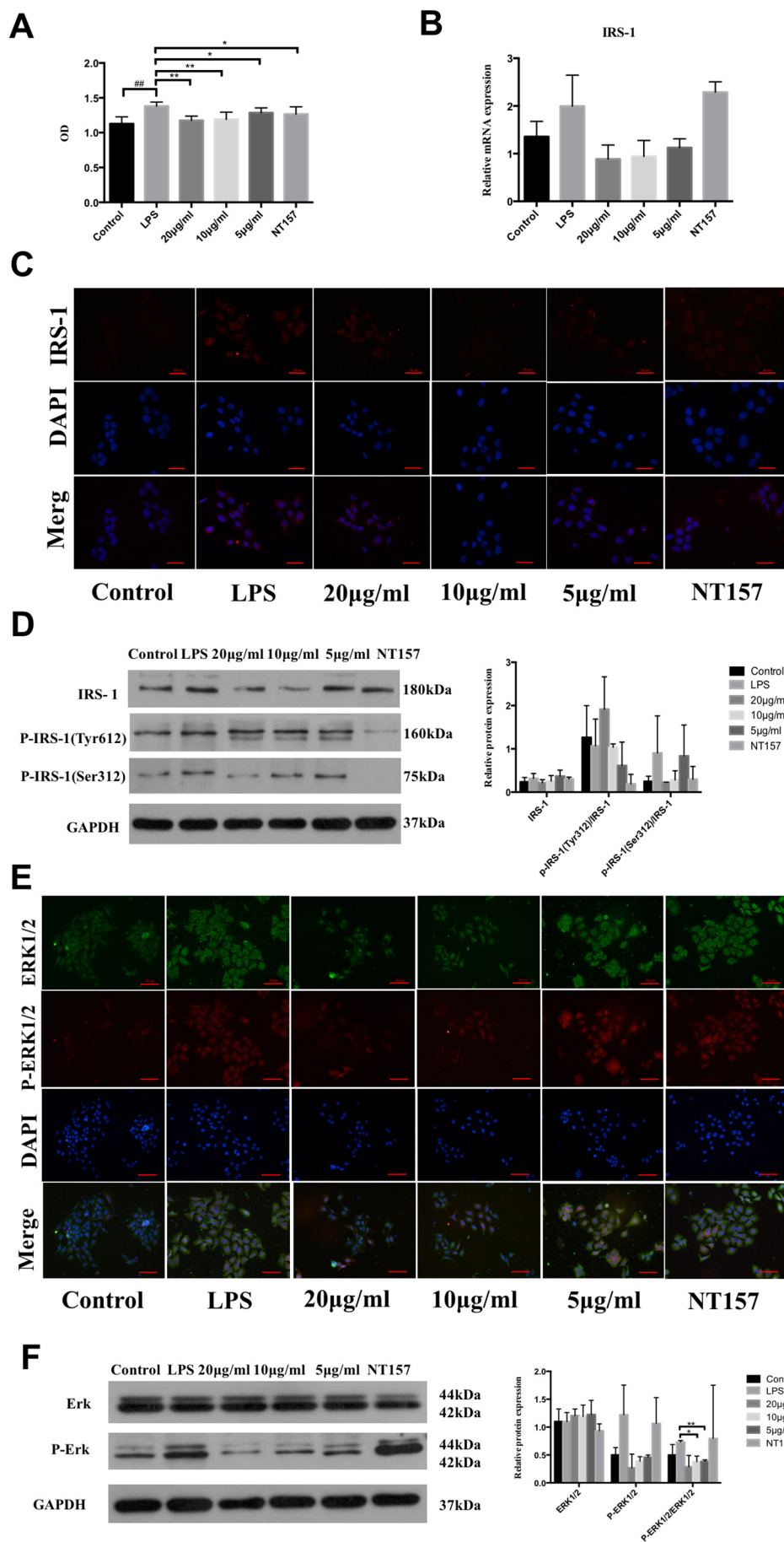


**Fig. 7.** Expression of IRS-1, p-IRS-1, ERK1/2, and p-ERK in HaCaT treated with LPS. (A) OD values in HaCaT stimulated with LPS for 24 h. Values are presented as mean ± SD (n = 6). \**p* < 0.05 and \*\**p* < 0.01 vs the model group; #*p* < 0.05 and ##*p* < 0.01 vs the control group. (B) The relative levels of IRS-1 gene expression in vitro were determined by RT-qPCR. Graphs indicate the mean ± SD for each group (n = 3). \**p* < 0.05 and \*\**p* < 0.01 vs the model group; \**p* < 0.05 and \*\**p* < 0.01 vs the model group; #*p* < 0.05 and ##*p* < 0.01 vs the control group. (C) Immunofluorescence (IF, ×200) images of IRS-1 in HaCaT. IRS-1 (red), DAPI (blue) and merge. Scale bar = 50 µm. (D) Protein levels of IRS-1, p-IRS (Tyr612) and p-IRS (Ser312) in HaCaT. Values are presented as mean ± SD of IRS-1, p-IRS (Tyr612)/IRS-1 and p-IRS (Ser312)/IRS-1 (n = 3), to indicate the phosphorylation levels of the different sites of IRS-1. \**p* < 0.05 and \*\**p* < 0.01 vs the model group; #*p* < 0.05 and ##*p* < 0.01 vs the control group. (E) Immunofluorescence (IF, ×200) images of ERK1/2 and p-ERK1/2 in HaCaT. ERK1/2 (green), p-ERK1/2 (red), DAPI (blue) and merge. Scale bar = 50 µm. (F) Protein levels of ERK1/2, p-ERK1/2 and the ratio of p-ERK1/2 to ERK1/2 in HaCaT. Values are presented as mean ± SD (n = 3). \**p* < 0.05 and \*\**p* < 0.01 vs the model group; #*p* < 0.05 and ##*p* < 0.01 vs the control group. (For interpretation of the references to color in this figure legend, the reader is referred to the web version of this article.)

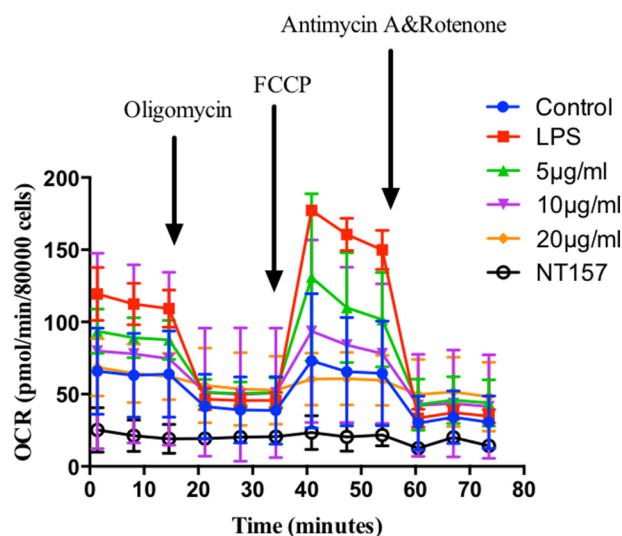


**Fig. 8.** Effect on respiration in HaCaT cells treated with LPS. OCR of HaCaT cells exposed sequentially to each modulator for mitochondrial activity (oligomycin, FCCP and Antimycin and Rotenone) in the presence of different concentrations of Hes for 24 h.

reduce IGF1R-associated survival signaling [38]. Our study demonstrated that NT157 could inhibit the proliferation of LPS-induced HaCaT cells after 48 h of treatment. However, NT157 was less potent compared to Hes. Although NT157 could suppress IRS-1 protein expression in LPS-induced HaCaT cells, it had no effect on IRS-1 gene expression. In addition, the inhibition of ERK1/2 phosphorylation was lower in LPS-induced HaCaT cells. Hence, we believe that IRS-1 inhibition alone does not completely reverse hyperproliferation of epidermal cells observed psoriasis. On the other hand, Hes could reduce IRS-1 serine phosphorylation, promote tyrosine phosphorylation and inhibit ERK-1/2 phosphorylation to restore IRS-1 levels. Finally, IRS-1 has many phosphorylation sites which had different effects on it [32,33]. In this experiment, we mainly focused on the Ser312 and Tyr612 loci of IRS-1. Future studies we will explore to the Hes effect on upstream and downstream of IRS-1, especially others loci in IRS-1. In vitro, we tried to add the DMEM (cell culture medium containing 4500 mg/L glucose) to LPS-stimulated HaCaT cells. But we did not find any difference between MEM-cultured cells in cell proliferation. The following work should be performed in mice with psoriasis that are concurrently IR or overweight to demonstrate its therapeutic benefit in regulating metabolism and treating psoriasis.

## 5. Conclusion

Based on the results from this study, Hes was found to inhibit PASI, secretion of pro-inflammatory factors in skin lesions, and reduce excessive epidermal proliferation and differentiation. It may play a therapeutic role in serum metabolic disorders and skin lesions, and hence improve the symptoms of psoriasisform dermatitis. Hes also affected aerobic respiration in keratinocytes, inhibited the phosphorylation of IRS-1 Ser312 and dephosphorylation of Tyr612 in keratinocytes, restored IRS-1 function and suppressed high expression of ERK1/2, thereby inhibiting keratinocyte proliferation. All these suggest that Hes plays a therapeutic role in psoriasis.

## Ethics approval for animal experiments

All animal experiments were conducted in strict accordance with the Guidelines for the Care and Use of Laboratory Animals published by the Scientific Committee of Beijing Institute of Traditional Chinese Medicine.

## Availability of data and materials

Access to materials and data will be granted upon reasonable request to the corresponding author.

## Conflicts of interest

The authors declare no conflicts of interest.

## Funding

This work was supported by grants from the National Natural Science Foundation of China (81603630, 81873119, 81573974).

## Authors' contributions

All authors read and approved the final manuscript.

## Acknowledgments

This work was supported by grants from the National Natural Science Foundation of China (81603630, 81873119, 81573974).

## Appendix A. Supplementary data

Supplementary data to this article can be found online at <https://doi.org/10.1016/j.lfs.2019.01.019>.

## References

- [1] F.O. Nestle, D.H. Kaplan, J. Barker, Psoriasis, *N. Engl. J. Med.* 361 (2009) 496–509.
- [2] W.H. Boehncke, Etiology and pathogenesis of psoriasis, *Rheum. Dis. Clin. N. Am.* 41 (4) (2015) 665–675.
- [3] I. Grozdev, N. Korman, N. Tsankov, Psoriasis as a systemic disease, *Clin. Dermatol.* 32 (3) (2014) 343–350.
- [4] B.B. Davidovici, N. Sattar, P.C. Jörg, et al., Psoriasis and systemic inflammatory diseases: potential mechanistic links between skin disease and co-morbid conditions, *J. Investig. Dermatol.* 130 (7) (2010) 1785–1796.
- [5] L. Naldi, L. Chatenoud, D. Linder, et al., Cigarette smoking, body mass index, and stressful life events as risk factors for psoriasis: results from an Italian case-control study, *J. Investig. Dermatol.* 125 (1) (2005) 61–67.
- [6] L. Barrea, N. Balato, C. Di Somma, et al., Nutrition and psoriasis: is there any association between the severity of the disease and adherence to the Mediterranean diet? *J. Transl. Med.* 13 (1) (2015).
- [7] M. Napolitano, M. Megna, G. Monfrecola, Insulin resistance and skin diseases, *Sci. World J.* 2015 (2015) 479–354.
- [8] C. Buerger, B. Richter, K. Woth, et al., Interleukin-1 $\beta$  interferes with epidermal homeostasis through induction of insulin resistance: implications for psoriasis pathogenesis, *J. Investig. Dermatol.* 132 (9) (2012) 2206–2214.
- [9] Huijuan Ming, Xiupu Shi, Zhonglin Yang, Effect of hesperidin on glucose metabolism in insulin resistant HepG2 cells, *Northwest Pharm. J.* 28 (3) (2013) 278–282.
- [10] A. Roohbakhsh, H. Parhiz, F. Soltani, et al., Molecular mechanisms behind the biological effects of hesperidin and hesperetin for the prevention of cancer and cardiovascular diseases, *Life Sci.* 124 (2015) 64–74.
- [11] R. Li, J. Li, L. Cai, et al., Suppression of adjuvant arthritis by hesperidin in rats and its mechanisms, *J. Pharm. Pharmacol.* 60 (2) (2008) 221–228.
- [12] G. Kaur, N. Tirkey, K. Chopra, Beneficial effect of hesperidin on lipopolysaccharide-induced hepatotoxicity, *Toxicology* 226 (2–3) (2006) 152–160.
- [13] S. Kobayashi, S. Tanabe, Evaluation of the anti-allergic activity of Citrus unshiu using rat basophilic leukemia RBL-2H3 cells as well as basophils of patients with seasonal allergic rhinitis to pollen, *Int. J. Mol. Med.* 17 (3) (2006) 511–515.
- [14] A. Malhotra, N. Shafiq, S. Rajagopalan, et al., Thiazolidinediones for plaque psoriasis: a systematic review and meta-analysis, *Evid. Based Med.* 17 (6) (2012) 171–176.
- [15] N.K. Salam, T.H. Huang, B.P. Kota, et al., Novel PPAR-gamma agonists identified from a natural product library: a virtual screening, induced-fit docking and biological assay study, *Chem. Biol. Drug Des.* 71 (2008) 57–70.
- [16] Y. Nagashio, Y. Matsuura, J. Miyamoto, et al., Hesperidin inhibits development of atopic dermatitis-like skin lesions in NC/Nga mice by suppressing Th17 activity, *J. Funct. Foods* 5 (4) (2013) 1633–1641.
- [17] C.C. Lin, J.J. Wu, Y.G. Pan, et al., Gold lotion from citrus peel extract ameliorates imiquimod-induced psoriasis-like dermatitis in murine, *J. Sci. Food Agric.* 24 (2018).
- [18] L. van der Fits, S. Mourits, J.S. Voerman, et al., Imiquimod-induced psoriasis-like skin inflammation in mice is mediated via the IL-23/IL-17 axis, *J. Immunol.* 182 (2009) 5836–5845.

- [19] Sristi Lakshmi, Amiya Nath, Carounanidy Udayashankar, Metabolic syndrome in patients with psoriasis: a comparative study, *Indian Dermatol. Online J.* 5 (2) (2014) 132–137.
- [20] I. Topić, D. Simić, Prevalence of metabolic syndrome in patients with psoriasis at Mostar Clinical Hospital, *Acta Clin. Croat.* 52 (1) (2013) 53–58.
- [21] J.J. Wu, B.E. Strober, P.R. Hansen, et al., Effects of tofacitinib on cardiovascular risk factors and cardiovascular outcomes based on phase III and long-term extension data in patients with plaque psoriasis, *J. Am. Acad. Dermatol.* 75 (5) (2016) 897–905.
- [22] R. Li, P. Krishnamoorthy, A. Raper, et al., Psoriasis is associated with decreased adiponectin levels beyond cardiovascular and metabolic risk factors, *Endocr. Abstr.* 29 (2012) 338.
- [23] M. Gyldenløve, H. Storgaard, J.J. Holst, et al., Patients with psoriasis are insulin resistant, *J. Am. Acad. Dermatol.* 72 (4) (2015) 599–605.
- [24] M.E. Farhangian, S.R. Feldman, Immunogenicity of biologic treatments for psoriasis: therapeutic consequences and the potential value of concomitant methotrexate, *Am. J. Clin. Dermatol.* 16 (4) (2015) 285–294.
- [25] Y. Wang, H. Yu, J. Zhang, et al., Hesperidin inhibits HeLa cell proliferation through apoptosis mediated by endoplasmic reticulum stress pathways and cell cycle arrest, *BMC Cancer* 12 (15) (2015) 682.
- [26] M. Hou, M. Man, W. Man, et al., Topical hesperidin improves epidermal permeability barrier function and epidermal differentiation in normal murine skin, *Exp. Dermatol.* 21 (2012) 337–340.
- [27] H. Parhiz, A. Roohbakhsh, F. Soltani, et al., Antioxidant and anti-inflammatory properties of the citrus flavonoids hesperidin and hesperetin: an updated review of their molecular mechanisms and experimental models, *Phytother. Res.* 29 (3) (2015) 323–331.
- [28] Dariush Haghmorad, Mohammad Bagher Mahmoudi, Zohreh Salehipour, et al., Hesperidin ameliorates immunological outcome and reduces neuroinflammation in the mouse model of multiple sclerosis, *J. Neuroimmunol.* 302 (2017) 23–33.
- [29] H. Takahashi, M. Ibe, S. Nakamura, et al., Extracellular regulated kinase and c-Jun N-terminal kinase are activated in psoriatic involved epidermis, *J. Dermatol. Sci.* 30 (2) (2002) 94–99.
- [30] I. Haase, R.M. Hobbs, M.R. Romero, et al., A role for mitogen-activated protein kinase activation by integrins in the pathogenesis of psoriasis, *J. Clin. Invest.* 108 (4) (2001) 527–536.
- [31] S. Colin, B. Darné, A. Kadi, et al., The antiangiogenic insulin receptor substrate-1 antisense oligonucleotide aganirsén impairs AU-rich mRNA stability by reducing 14-3-3 $\beta$ -tristetraprolin protein complex, reducing inflammation and psoriatic lesion size in patients, *J. Pharmacol. Exp. Ther.* 349 (1) (2014) 107–117.
- [32] R.J. Walker, N.M. Anderson, S. Bahouth, et al., Silencing of insulin receptor substrate-1 increases cell death in retinal Müller cells, *Mol. Vis.* 18 (2012) 271–279.
- [33] S.K. Bose, S. Shrivastava, K. Meyer, et al., Hepatitis C virus activates the mTOR/S6K1 signaling pathway in inhibiting IRS-1 function for insulin resistance, *J. Virol.* 86 (11) (2012) 6315–6322.
- [34] C.A. Aspinwall, W.J. Qian, M.G. Roper, et al., Roles of insulin receptor substrate-1, phosphatidylinositol 3-kinase, and release of intracellular Ca<sup>2+</sup> stores in insulin stimulated insulin secretion in  $\beta$  cells, *J. Biol. Chem.* 275 (29) (2000) 22331–22338.
- [35] M. Rajappa, S. Rathika, M. Munisamy, et al., Effect of treatment with methotrexate and coal tar on adipokine levels and indices of insulin resistance and sensitivity in patients with psoriasis vulgaris, *J. Eur. Acad. Dermatol. Venereol.* 29 (1) (2015) 69–76.
- [36] M. Coban, L. Tasli, S. Turgut, et al., Association of adipokines, insulin resistance, hypertension and dyslipidemia in patients with psoriasis vulgaris, *Ann. Dermatol.* 28 (1) (2016) 74.
- [37] I. Bulur, E.H. Kaya, E. Kocatürk, et al., The role of irisin in the relationship between psoriasis and insulin resistance, *G. Ital. Dermatol. Venereol.* 153 (4) (2018) 477–482.
- [38] H. Reuveni, E. Flashner-Abramson, L. Steiner, et al., Therapeutic destruction of insulin receptor substrates for cancer treatment, *Cancer Res.* 73 (14) (2013) 4383–4394.